Nanoscale Res Lett
DOI 10.1007/s11671-009-9276-z

NANO EXPRESS

Epitaxial Catalyst-Free Growth of InN Nanorods on *c*-Plane Sapphire

I. Shalish · G. Seryogin · W. Yi · J. M. Bao · M. A. Zimmler · E. Likovich · D. C. Bell · F. Capasso · V. Narayanamurti

Received: 24 December 2008 / Accepted: 9 February 2009
© to the authors 2009

Abstract We report observation of catalyst-free hydride vapor phase epitaxy growth of InN nanorods. Characterization of the nanorods with transmission electron microscopy, and X-ray diffraction show that the nanorods are stoichiometric 2H–InN single crystals growing in the [0001] orientation. The InN rods are uniform, showing very little variation in both diameter and length. Surprisingly, the rods show clear epitaxial relations with the *c*-plane sapphire substrate, despite about 29% of lattice mismatch. Comparing catalyst-free with Ni-catalyzed growth, the only difference observed is in the density of nucleation sites, suggesting that Ni does not work like the typical vapor–liquid–solid catalyst, but rather functions as a nucleation promoter by catalyzing the decomposition of ammonia. No conclusive photoluminescence was observed from single nanorods, while integrating over a large area showed weak wide emissions centered at 0.78 and at 1.9 eV.

Keywords InN · Nanorods · Nanowires · Epitaxial growth · Sapphire · Catalyst-free · Ni

I. Shalish (✉) · G. Seryogin · W. Yi · J. M. Bao · M. A. Zimmler · E. Likovich · D. C. Bell · F. Capasso · V. Narayanamurti
Harvard University, Cambridge, MA 02138, USA
e-mail: shalish@seas.harvard.edu

I. Shalish
Ben Gurion University, Beer Sheva, Israel

Present Address:
J. M. Bao
University of Houston, Houston, TX 77004, USA

Introduction

InN marks the lower bandgap limit achievable within the group III-nitride semiconductor family. To date, it has also been the most difficult-to-grow among that family, mainly because at its growth temperature, InN decomposes almost as readily as ammonia. Incorporation of In into GaN has also been difficult, especially at high In percentage, due to the large difference in growth temperature between InN and GaN [1]. An even more challenging scenario is encountered when one attempts a catalytic growth of InN nanowires. Catalytic growth is commonly preferred, for it allows control of size and position of the wires. A catalyst of choice is one that is inert and can liquefy, if not as a pure element, at least by eutectic reaction with another element, below the growth temperature. The most common choice is Au. Au can melt eutectically in reaction with Si but not as well on sapphire, the more common substrate for nitrides. Furthermore, nitrogen is claimed to be poorly soluble in Au [2]. Growth with Au catalyst has been reported [3], but due to its relatively low efficiency, it typically requires large flow of ammonia. In many studies, catalyzed nitride nanowires are grown with Ni [4, 5]. In this paper, we report an observation of catalyst-free epitaxial growth of remarkably size-uniform and vertically-aligned InN nanorods on *c*-plane sapphire. We compare this growth to Ni catalyzed growth under the same conditions and suggest that a growth mechanism other than vapor–liquid–solid (VLS) may be responsible for the observed uniformity.

Experimental Details

Growth of InN on *c*-plane sapphire was carried out in a custom designed HVPE reactor. The reactor consists of

Published online: 27 February 2009

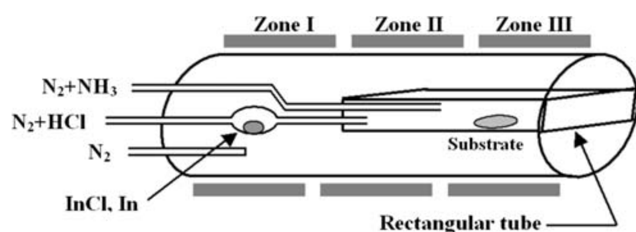

Fig. 1 Horizontal HVPE reactor used for InN nanowire growth

75 mm quartz tube, placed in a three-zone Mellen horizontal furnace. Quartz insert with a rectangular cross-section is employed to produce laminar flow in the growth zone and to suppress turbulence (Fig. 1). Two of the heating zones are used for hydride reactions of column-III-metals with HCl gas. In this work, only indium was used as the source metal and the InCl was formed in a direct reaction between molten In and HCl gas diluted with N_2. The resulting Indium chloride is formed in an internal quartz tube (10 mm cross section) at 500 °C and is carried in its dedicated tube into the rectangular part. The third zone is the growth zone that was kept at 550 °C during the process. Ammonia is delivered to the growth zone via separate 10 mm diameter quartz tube, and the InCl gas reacts with ammonia to form InN. The growth was carried out either with 1.5 nm of thermally deposited Ni as catalyst or without catalyst.

Process gasses were exhausted through a Lab Guard wet scrubbing system. The growth was carried out at atmospheric pressure. Ultra high purity Ar was used as a carrier gas. Typical carrier flow was 3000 sccm, HCl and NH3 flows were 1–10 and 50–200 sccm, respectively. The efficiency of ammonia decomposition drops with temperature, and is rather low at the InN growth temperatures. For this reason, the growth of InN requires a relatively high flow of ammonia [6]. The growth was estimated to be at a rate of ~45 nm/min and was carried out for 30 min.

Scanning electron microscopy was carried out in a LEO (Zeiss) 982 FEG-SEM Field Emission Gun Scanning Electron Microscope with a Noran thin-window electron-dispersive spectroscopy (EDS) detector. Tunneling electron microscopy (TEM) was performed using a JEOL 2010-FEG-TEM/STEM operated at 200 keV with attached EDAX thin-window detector. Photoluminescence (PL) was excited at room temperature using a HeCd laser (325 nm, 8 mW). The emitted luminescence was dispersed by a monochromator, filtered, and sensed using a Si CCD camera.

Results

Vertically aligned nanorods grew over the entire sample area at density varying roughly between 1 and 2 rods per μm^2 (Fig. 2, top-left panel). The rods are strikingly uniform in size, with thickness of 374 ± 21 nm (standard deviation 5.6 %) and length of 1725 ± 56 nm (standard deviation 3.2 %) (Fig. 2, top-right panel). We believe that the higher standard deviation in the width value is an artifact resulting from ill-defined diameter of hexagonal cross-section rod. Samples deposited with Ni catalyst produced the same size, length, and shape of rods, except for a much higher nucleation density of 6–8 rods per μm^2 (Fig. 2, bottom panel), effectively fusing the nanorods into a continuous layer.

Close examination of adjacent rods (Fig. 3) reveals that the rods are aligned to one another, i.e., no relative rotations observed around the growth axis, which suggests that the rods have epitaxial relations with the substrate. While the rods appear to possess sixfold symmetry, they actually show 12 facets that appear as two six-faceted rods grown into one another from the two ends of the wire toward the middle. However, selected area diffractions did not show any difference between adjacent facets. Electron dispersive spectroscopy shows that the main elements are In and N (Fig. 4). No other element could be conclusively identified.

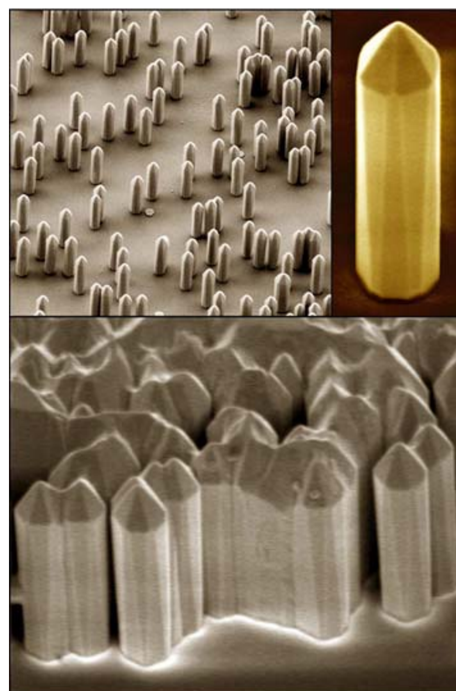

Fig. 2 Catalyst-free (top) and Ni-catalyzed (bottom) InN nanorods grown on *c*-plane sapphire substrate. The images (SEM) were taken at various degrees of tilt (~45°). Color was added to increase contrast. The nanorod placement is random, but the size is outstandingly uniform. The vertical alignment testifies to the existence of epitaxial relations between the *c*-plane sapphire substrate and the InN nanorods. Each nanorod is 1725-nm-high and 375-nm-wide on the average. Image width: top-left: 10.5 µm, top-right: 550 nm, bottom: 3.33 µm

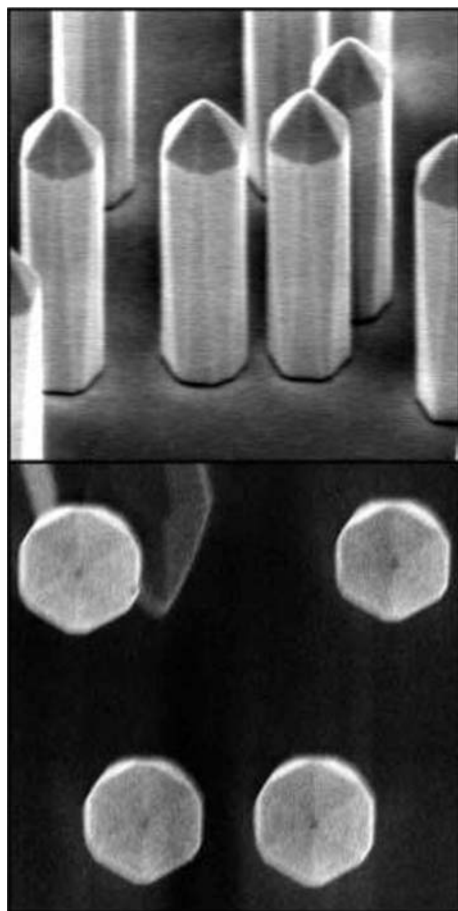

Fig. 3 Vertical (top-panel) and rotational (bottom-panel) allignment between separate InN nanorods testifying epitaxial relations with the *c*-plane sapphire substrate. The top SEM image was taken at about 42° tilt. The bottom image was taken without tilt. Image width: top: 2 μm, bottom: 1.5 μm

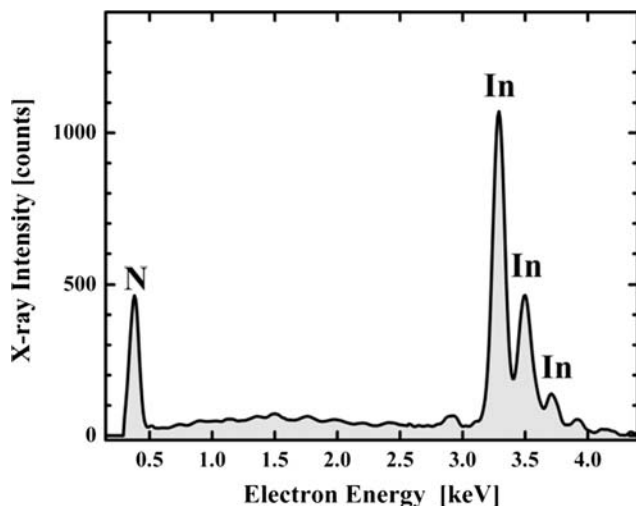

Fig. 4 Energy dispersive spectroscopy of a layer of fused InN nanorods, showing emission from In, and N

Specifically, we could not detect any Ni on the rod tip as in the classic case of VLS catalysis [7].

$2\Theta-\omega$ symmetric X-ray diffraction (Fig. 5, top) main peaks are clearly identified as Al_2O_3(0006), InN(0002), and InN(0004), which confirms what is already suggested in the SEM image, that the rods adopt the *c*-orientation of their sapphire substrate. Zooming into the background of the diffraction spectrum (Fig. 5, bottom) reveals InN$(10\bar{1}1)$ peak, diffracted by the sloped sides of the tip, as well as InN$(10\bar{1}2)$ and InN$(10\bar{1}3)$ and a peak of InN$(10\bar{1}0)$ (and a weaker InN$(20\bar{2}0)$) which are likely to originate from a small percentage of uprooted rods laying on their side. Neither free Ni nor its chlorides, nitrides, or oxides were detected.

Figure 6 shows a single InN nanorod on a TEM grid and the corresponding selective area diffraction. The diffraction is from the $[10\bar{1}0]$ zone axis, and provides another confirmation of the [0001] growth orientation. High-resolution imaging was not possible due to the thickness of the rods and the low decomposition temperature of InN, but electron diffraction from a larger selected area diffraction aperture confirms that the rods are single crystals. STEM/EDS was used to monitor Ni in Ni catalyzed rods. Ni signal was below the noise limit. This suggests that Ni is either

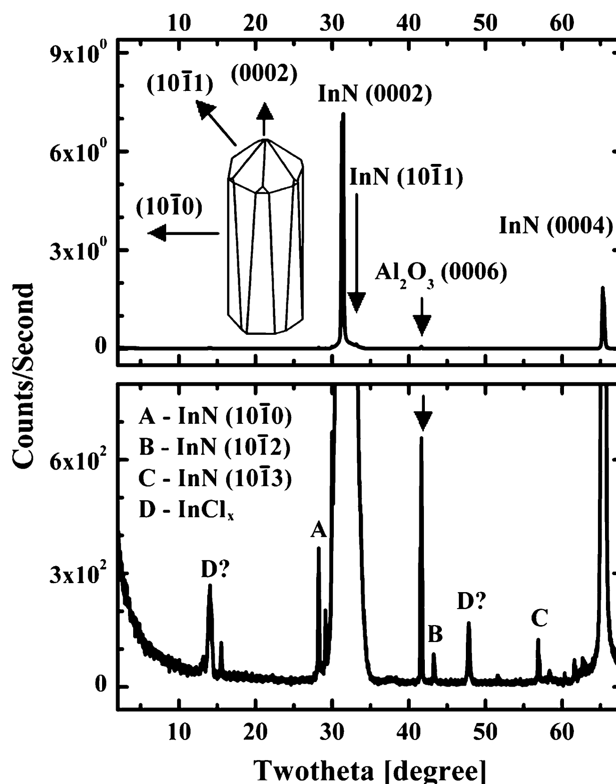

Fig. 5 Symmetric $2\Theta-\omega$ X-ray diffraction of vertically aligned InN nanorods grown on *c*-plane sapphire (top) and zoomed-in view of the background diffraction (bottom)

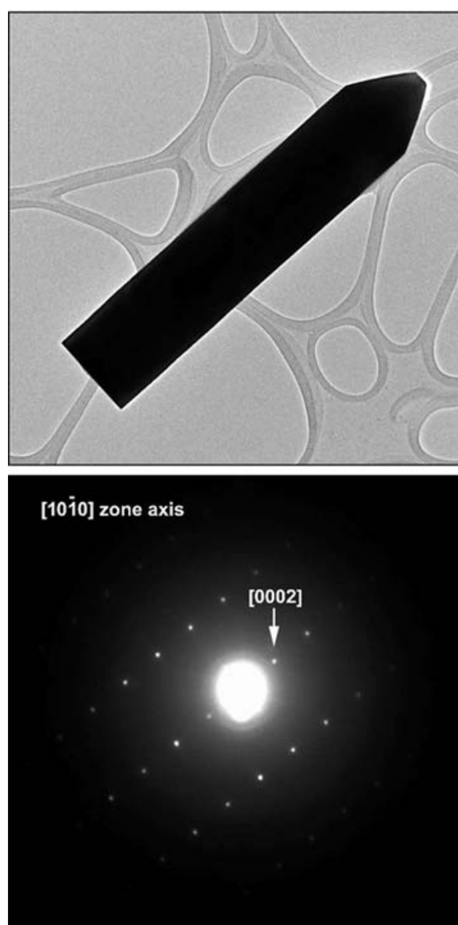

Fig. 6 TEM selective area diffraction from the [10$\bar{1}$0] zone axis of an individual nanorod. The diffraction provides another confirmation of the [0001] growth orientation

etched away by the HCl product of the HVPE reaction or remains at the substrate interface.

Photoluminescence measurements were carried out at room temperature. Photoluminescence, integrating emissions from a wide area, is shown in Fig. 7. It combines the results of two measurements: one, with Ar laser pumping and InGaAs detector for the infrared range, and another using He–Cd laser pumping and Si detector for the visible range. It shows weak emission centered at 0.78 eV and even weaker emission peak centered at 1.9 eV. Both these emissions have been suggested to be InN band edge emission. The commonly suggested (though not conclusively established) explanation on these emissions today is for the 0.7–0.8 eV to be the band edge of pure InN [8], and for the 1.9 eV to result from some presence of oxygen compounds, pulling the band edge up towards that of the In_2O_3($\sim$3.7 eV) [9]. However, no evidence for oxygen was present in EDS of individual rods, or for oxides in XRD of the entire sample. In the case of nanowires, it is always more instructive to obtain luminescence from an individual wire, in order to exclude background that often includes

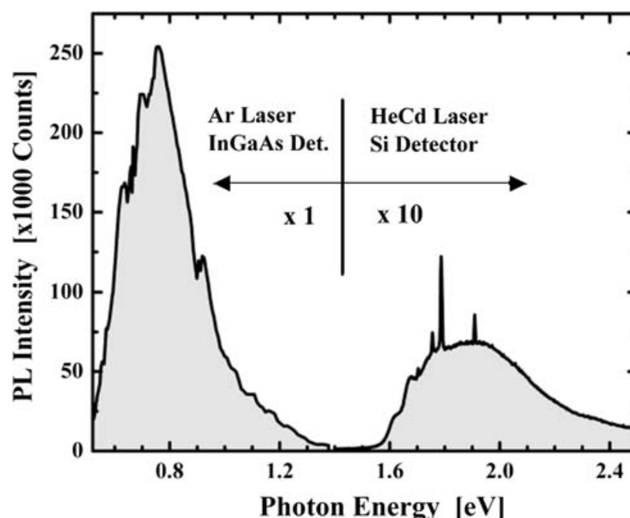

Fig. 7 Room temperature photoluminescence, integrating emissions over a wide area, combining results of two measurements: One, with Ar laser pumping and InGaAs detector for the infrared range, and another using He–Cd laser pumping and Si detector for the visible range. It shows week emission centered at 0.78 eV and even weaker emission peak centered at 1.9 eV

various defective particles. However, in our case, emission from individual nanorods was consistently below the noise level.

To assess the material resistivity, we carried out standard four-point probe sheet resistance measurement on continuous layers of fused nanorods grown using Ni catalyst. The measured sheet resistance of 55.5 Ohm/square, multiplied by the film thickness of 1.8 mm, yields 0.01 Ohm cm.

Discussion

Weak radiative recombination is not uncommon in narrow gap III–V semiconductors, especially when nanostructured. Possibly, the increased surface-to-volume ratio gives rise to enhanced effect of surface recombination. Since surface states are typically below the bandgap energy, and since our InGaAs detector was limited to 0.6 eV, our experiment was practically blind to any emission below 0.6 eV. Surface deep levels usually mean surface depletion. However, narrow gap III–V semiconductors, especially In-based, such as InAs and InSb, are known to have their surface Fermi level pinned above the conduction band, giving rise to surface accumulation layer [10]. The high density of accumulated electrons at the surface is a known cause for non-radiative recombination through Auger processes. Auger recombination has been shown to be the main non-radiative recombination mechanism in InGaAs semiconductor devices, having band gap energy in the range of

0.6–0.8 eV [11]. While the effectiveness of Auger processes in InN is still under debate [12, 13], it is known to strongly depend on the doping. The resistivity of our material (0.01 Ohm cm) seems low enough to make this mechanism important.

While PL does not provide a conclusive identification of InN, both in general and specifically in our experiment, our X-ray and TEM/selective area diffraction data present a clear picture of *c*-oriented material growth, with EDS clearly identifying the main elements as indium and nitrogen. The lack of Ni signal in EDS spectra does not exclude Ni incorporation within the InN rods, but conclusively confirms its absence at the rod tip, at the typical VLS catalyst placement, commonly observed in VLS growth.

Ni does not melt (not even by eutectic reaction with sapphire or aluminum) at the growth temperature range [14]. Therefore, it is quite clear that if the growth still takes place by vapor–liquid–solid mode, the only available liquid metal in the system is that of the group III metal, i.e., the growth is most likely self-catalyzed by the group III metal [15]. Nonetheless, we observe a clear increase in nucleation density in *c*-plane sapphire samples deposited with Ni compared with bare samples grown simultaneously at the same run (comparing the top and bottom panels of Fig. 2). We therefore suggest that Ni serves as a *nucleation promoter* possibly by virtue of its ability to catalyze ammonia decomposition [16–20]. This type of catalysis is less likely to yield diameter control, as does the common VLS-mode catalyst, but may easily explain the order of magnitude denser nucleation of rods we observe in the presence of Ni. Further structural studies, e.g., cross-sectional TEM of the nucleation phase of the growth, could shed more light on the details of the Ni role.

Self-VLS-catalysis, e.g., with In, as is possible in our case, is also unlikely to provide any control, as the metal vapor is being showered all over the sample continuously through the growth, unlike the case of VLS, where the size and placement of catalyst droplets is well-defined at the beginning of the growth and is relatively stable through the growth. Hence the outstanding diameter uniformity that we observe cannot be explained by the VLS model and does not seem to be related to the Ni catalyst either.

Another form of outstanding uniformity is the rotational alignment of the rods. Such alignment would only be possible under epitaxial relations. However, this is rather surprising considering a lattice mismatch of 29% between InN and sapphire, known to produce structural defects (misfit dislocations) in films. Typically in such cases, the wire structure shows a wider cone shaped base, where the strain is gradually relieved [21, 22]. No such effect, or any other effect of strain has been observed in our case. In a theoretical work, Ertekin et al. showed that nanowire heterostructures are more effective at relieving mismatch strain coherently compared with films. The critical diameter for coherent growth of nanowires on lattice-mismatched substrates was predicted to be up to one order of magnitude larger than that of thin film growth [23]. Yet, most of the published works on growth of InN nanorods on *c*-plane sapphire typically observe random orientations emanating from each nucleus with no clear expitaxial relation to the substrate [24–26].

Epitaxial growth of InN on *c*-plane sapphire has been explored [27, 28]. However, to date, an intermediate layer of AlN (often formed by nitridation of the sapphire substrate) or a bilayer AlN\GaN have always been used to bridge the mismatch and reduce the defect formation. In our case, we did not perform any intentional pretreatment. Nitridation is highly unlikely to have taken place at 550 °C. Unintentional In_2O_3 is also unlikely to be able to bridge between InN and sapphire, because In_2O_3 is of cubic symmetry. Hence, it seems highly likely that the epitaxial relations we observed were direct, although the details of the actual mechanism require further investigation.

Conclusion

Our observation suggests that InN may establish direct epitaxial relation with *c*-plane sapphire and may also form nanoscale fibers without extrinsic catalyst. Use of Ni as catalyst is only seen to increase the nucleation density and is therefore suggested to work as nucleation promoter by catalyzing ammonia decomposition.

Acknowledgments This work was supported by the National Science Foundation through grant # ECS-0322720. I.S. acknowledges a Converging Technologies personal grant from the Israeli Science Foundation - VATAT.

References

1. A.G. Bhuiyan, A. Hashimoto, A. Yamamoto, J. Appl. Phys. **94**, 2779 (2003)
2. H. Okamoto, T.B. Massalski, J. Phase Equilib. **5**, 381 (1984)
3. C.W. Hsu, A. Ganguly, C.H. Liang, Y.T. Hung, C.T. Wu, G.M. Hsu, Y.F. Chen, C.C. Chen, K.H. Chen, L.C. Chen, Adv. Funct. Mater. **18**, 938 (2008)
4. X.F. Duan, C.M. Lieber, J. Am. Chem. Soc. **122**, 188 (2000)
5. J. Zhang, L. Zhang, J. Vac, Sci. Technol. B **21**, 2415 (2003)
6. X.M. Cai, F. Yeb, S.Y. Jing, D.P. Zhang, P. Fan, E.Q. Xie, Appl. Surf. Sci. **255**, 2153 (2008)
7. R.S. Wagner, W.C. Ellis, Appl. Phys. Lett. **4**, 89 (1964)
8. H.Y. Chen, C.H. Shen, H.W. Lin, C.H. Chen, C.Y. Wu, S. Gwo, V.Y. Davydov, A.A. Klochikhin, Thin Solid Films **515**, 961 (2006)
9. K.S.A. Butcher, T.L. Tansley, Superlattice. Microst. **38**, 1 (2005)
10. T. Stoica, R.J. Meijers, R. Calarco, T. Richter, E. Sutter, H. Lueth, Nano Lett. **6**, 1541 (2006)
11. W.K. Metzger, M.W. Wanlass, R.J. Ellingson, R.K. Ahrenkiel, J.J. Carapella, Appl. Phys. Lett. **79**, 3272 (2001)

12. R. Ascazubi, I. Wilke, S. Cho, H. Lu, W.J. Schaff, Appl. Phys. Lett. **88**, 112111 (2006)
13. T.-R. Tsai, C.-F. Chang, S. Gwo, Appl. Phys. Lett. **90**, 252111 (2007)
14. T.B. Massalski, *Binary Alloy Phase Diagrams*, 2nd edn. (ASM International, Bilthoven, 1990
15. B.S. Simpkins, L.M. Ericson, R.M. Stroud, K.A. Pettigrew, P.E. Pehrsson, J. Cryst. Growth **290**, 115 (2006)
16. M. Grunze, M. Golze, R.K. Driscoll, P.A. Dowben, J. Vac. Sci. Technol. **18**, 611 (1981)
17. M. Grunze, P.A. Dowben, C.R. Brundle, Surf. Sci. **128**, 311 (1983)
18. I.C. Bassignana, K. Wagemann, J. Kueppers, G. Ertl, Surf. Sci. **175**, 22 (1986)
19. D. Chrysostomou, J. Flowers, F. Zaera, Surf. Sci. **439**, 34 (1999)
20. S.F. Yina, B.Q. Xub, X.P. Zhouc, C.T. Au, Appl. Catal. A Gen. **277**, 1 (2004)
21. T. Martensson, C. Patrik, T. Svensson, B.A. Wacaser, M.W. Larsson, W. Seifert, K. Deppert, A. Gustafsson, L.R. Wallenberg, L. Samuelson, Nano Lett. **4**, 1987 (2004)
22. H.-M. Kim, D.S. Kim, Y.S. Park, D.Y. Kim, T.W. Kang, K.S. Chung, Adv. Mater. **14**, 991 (2002)
23. E. Ertekin, P.A. Greaney, D.C. Chrzan, T.D. Sands, J. Appl. Phys. **97**, 114325 (2005)
24. A. Syrkin, A. Usikov, V. Soukhoveev, O. Kovalenkov, V. Ivantsov, V. Dmitriev, C. Collins, E. Readinger, N. Shmidt, V. Davydov, S. Nikishin, V. Kuryatkov, D. Song, D. Rosenbladt, M. Holtz, Phys. Status Solidi **3**, 1444 (2006)
25. O. Kryliouk, H.J. Park, Y.S. Won, T. Anderson, A. Davydov, I. Levin, J.H. Kim, J.A. Freitas Jr., Nanotechnology **18**, 135606 (2007)
26. H.J. Park, O. Kryliouk, T. Anderson, D. Khokhlov, T. Burbaev, Physica E **37**, 142 (2007)
27. J. Ohta, H. Fujioka, T. Honke, M. Oshima, Thin Solid Films **457**, 109 (2004)
28. C.J. Lua, X.F. Duan, H. Lu, W.J. Schaff, J. Mater. Res. **21**, 1693 (2006)